Precision Agric (2016) 17:183–199
DOI 10.1007/s11119-015-9415-8

Early season weed mapping in sunflower using UAV technology: variability of herbicide treatment maps against weed thresholds

Francisca López-Granados[1] · Jorge Torres-Sánchez[1] · Angélica Serrano-Pérez[1] · Ana I. de Castro[1] · Fco.-Javier Mesas-Carrascosa[2] · José-Manuel Peña[1]

Published online: 20 August 2015

Abstract Site-specific weed management is defined as the application of customised control treatments only where weeds are located within the crop-field by using adequate herbicide according to weed emergence. The aim of the study was to generate georeferenced weed seedling infestation maps in two sunflower fields by analysing overlapping aerial images of the visible and near-infrared spectrum (using visible or multi-spectral cameras) collected by an unmanned aerial vehicle (UAV) flying at 30 and 60 m altitudes. The main tasks focused on the configuration and evaluation of the UAV and its sensors for image acquisition and ortho-mosaicking, as well as the development of an automatic and robust image analysis procedure for weed seedling mapping used to design a site-specific weed management program. The control strategy was based on seven weed thresholds with 2.5 steps of increasing ratio from 0 % (herbicide must be applied just when there is presence or absence of weed) to 15 % (herbicide applied when weed coverage >15 %). As a first step of the imagery analysis, sunflower rows were correctly matched to the ortho-mosaicked imagery, which allowed accurate image analysis using object-based image analysis [object-based-image-analysis (OBIA) methods]. The OBIA algorithm developed for weed seedling mapping with ortho-mosaicked imagery successfully classified the sunflower-rows with 100 % accuracy in both fields for all flight altitudes and camera types, indicating the computational and analytical robustness of OBIA. Regarding weed discrimination, high accuracies were observed using the multi-spectral camera at any flight altitude, with the highest (approximately 100 %) being those recorded for the 15 % weed threshold, although satisfactory results from 2.5 to 5 % thresholds were also observed, with accuracies higher than 85 % for both field 1 and field 2. The lowest accuracies (ranging from 50 to 60 %) were achieved with the visible camera at all flight altitudes and 0 %

✉ Francisca López-Granados
flgranados@ias.csic.es;
http://www.ias.csic.es/

[1] Institute for Sustainable Agriculture, CSIC, P.O. Box 4084, 14080 Córdoba, Spain

[2] Department of Graphic Engineering and Geomatics, University of Cordoba, Campus de Rabanales, 14071 Córdoba, Spain

weed threshold. Herbicide savings were relevant in both fields, although they were higher in field 2 due to less weed infestation. These herbicide savings varied according to the different scenarios studied. For example, in field 2 and at 30 m flight altitude and using the multi-spectral camera, a range of 23–3 % of the field (i.e., 77 and 97 % of area) could be treated for 0–15 % weed thresholds. The OBIA procedure computed multiple data which permitted calculation of herbicide requirements for timely and site-specific post-emergence weed seedling management.

Keywords Site-specific weed management (SSWM) · Mosaicked imagery · object-based-image-analysis (OBIA) · Remote sensing · Unmanned aerial vehicle (UAV) · Weed threshold

Introduction

Efficient and timely post-emergence weed control is a critical task in crop production because inappropriate weed management tends to reduce yield and increase the negative impacts on the environment. Inappropriate weed management is often related to incorrect herbicide use resulting from three main problems. The first is applying herbicides when weeds are not in the suitable phenological stage (generally when weeds have 4–6 true leaves, although this depends on specific weed species or group of species), the second is applying herbicides without considering any weed threshold (i.e., the weed infestation level above which a treatment is required (Swanton et al. 1999)), the third is broadcasting herbicides over the entire field, even when weed-free areas are present due to the usual weed patchy distribution (Jurado-Expósito et al. 2003, 2005). The first problem is usually addressed using the expert knowledge of farmers. The other two problems can be overcome by developing site-specific weed management (SSWM) strategies according to weed thresholds (Longchamps et al. 2014). These strategies may consist of both a single herbicide treatment to weed patches where a unique group of weeds is present (for example either grass or broadleaved weeds), or use of several herbicides according to the presence of different weed species or group composition, such as grass, broadleaved weeds or a specific problematic weed such as *Orobanche*-broomrape, which can be a serious problem in sunflower production (García-Torres et al. 1994; Molinero-Ruiz et al. 2014). Sunflower (*Helianthus annuus* L.) is the most important annual oilseed crop in southern Europe and the Black Sea region, with over 5 M ha grown annually (FAO 2015), of which 0.8 M ha are in Spain (MAGRAMA 2015). Weed control operations (either chemical or physical) using large agricultural machinery account for a significant proportion of production costs, create various agronomic problems (soil compaction and erosion) and represent a risk for environmental pollution. In this context, there is a demand for developing a timely, post-emergence, site-specific management program in order to reduce the issues associated with current weed control practices in sunflower and to comply with the European legislation and concerns (Regulation EC No 1107/2009; Directive 2009/128/EC; Horizon 2020).

To achieve these goals, it is necessary to generate the weed cover maps, which allow the translation of the spatial distribution of the weed infestation into site-specific herbicide treatment maps. As reported earlier, one of the main variables considered in the weed control decision process in sunflower is weed threshold, which is based on weed density or level of infestation (Castro-Tendero and García-Torres 1995; Carranza et al. 1995). If these weed cover or weed infestation maps are built using a grid design, a weed threshold can be

derived, which is the percentage of weed cover in every grid, above which a treatment is required. This threshold could be the baseline to generate the herbicide treatment maps. Remote sensing, together with proximal sensing, are now two of the principal sources of data to monitor weeds in a cost effective way. There are previous studies that have investigated weed detection and mapping in crops at late growth stages, e.g., flowering, using imagery from piloted airborne or satellite able to register visible and near-infrared information (Gutiérrez-Peña et al. 2008; De Castro et al. 2012, 2013). However, the images from these platforms have limited ability to detect weeds at the seedling stage due to their low spatial resolution. Other remote platforms, on the other hand, can generate the high spatial resolution imagery (pixel size $\leq$0.05 m) needed to map weeds at very early phenological stages, which can then be used to develop efficient post-emergence controls. Recent research emphasises the suitability of unmanned aerial vehicles (UAV) for this purpose (López-Granados 2011; Zhang and Kovacs 2012). A key component of a UAV is the versatility of the configuration of onboard sensors, flight altitude, flight planning, etc. The required parameters and their implications for the potential use of UAV in early weed detection have been reported by Torres-Sánchez et al. (2013). The main advantages of using UAV is that they can carry (even simultaneously) different sensors to record reflected energy at diverse spectral ranges according to each detection objective, fly at different altitudes to adjust the desired high spatial resolution and be programmed on demand at critical stages of crop growth. This is crucial when detecting weeds in crops for early post-emergence SSWM when crops and weeds are at the same early phenological stage and they show spectral and visual similarities.

As a result of collecting images with a very high spatial resolution, UAV images taken at low altitude cannot cover the entire study area. This causes the need to take a sequence of a percentage of forward (lateral) and side (longitudinal) overlapped imagery, which acquire a number of images per hectare depending on the flight altitude. These individual images must then be stitched together and ortho-rectified to create an accurately geo-referenced ortho-mosaicked image of the entire plot for further analysis and classification. Image mosaicking is a well-known task for integrating spatial data to assess and monitor disasters (Li et al. 2011), map archaeological sites (Lambers et al. 2007) or conduct high quality cadastral and urban planning (Haarbrink 2008) using local invariant features or ground control points to perform the aero-triangulation. However, the splicing image used to generate an ortho-image (also named ortho-mosaicked image) of herbaceous crops at early stages of phenological development presents serious difficulties due to the high repetitive pattern of these fields. In a recent work, our research group discussed a detailed procedure to produce accurate ortho-imagery with spatial resolutions from 0.0074 to 0.0247 m and representing the entire area of wheat fields (rows 0.15 m apart) by using UAV flying at low altitudes (Gómez-Candón et al. 2014). This work concluded that one of the crucial parameters for generating ortho-mosaicked imagery when mapping row crop environments is crop row alignment on both sides of the overlapped images. This issue was addressed and crop line continuity was preserved because overall spatial errors less than twice the spatial resolution were obtained. This methodology was very useful in the development of the objectives herein presented.

One of the intrinsic problems when processing very high spectral resolution imagery is that individual pixels do not capture the distinctiveness of the targets investigated, which generates a high intra-class spectral variability and, consequently, resulting in difficulties to achieve statistical separation. Segmentation is the process of dividing a digital image into multiple regions according to the proposed objective. For example, to discriminate weeds in a crop using UAV imagery, the segmentation would consist of multi-pixel regions

defined by crop, weeds and bare soil. That is, throughout the segmentation, spatially adjacent and spectrally homogeneous pixels would be grouped to create units named objects that contain more information than individual pixels, allowing for a more meaningful interpretation. This is the main idea behind the steps of the object-based-image-analysis (OBIA) procedure: (1) to automatically segment an image into objects, (2) to combine their spectral, contextual, morphological and hierarchical information, and (3) to classify the image by using them as the minimum information units (Blaschke 2010). Peña et al. (2013) developed an OBIA algorithm using single UAV imagery (not ortho-mosaicked imagery) for early detection of weeds in maize

As previously described, UAV ortho-mosaics are becoming an important tool for the development of site-specific weed prescription strategies because they can offer information on the entire study area and can detect small plants (crop and weeds) at early growth stages, which are not detected using other kinds of remote platforms with coarse spatial resolution (like satellite or conventional aerial platforms with which objects smaller than 0.20 m cannot be detected). Considering that highly accurate mosaics have been obtained working in wheat fields (Gómez-Candón et al. 2014), generation of ortho-mosaicked imagery for sunflower fields with 0.70 m row spacing seems to be a reasonable starting point for developing an early SSWM program, in which the relative location of weeds in proximity to the crop rows is a hypothesis for discriminating and mapping weed cover. Thus, the objectives of this work were to: (1) assess the optimal planning of UAV flights with respect to flight altitude and sensor type (visible vs visible + near-infrared cameras) for generating accurate ortho-imagery, (2) design and evaluate an OBIA procedure for mapping bare soil, crop-rows, weed-patches and weed-free zones using the ortho-mosaicked imagery, and (3) simulate several field-based scenarios according to different weed thresholds to evaluate the sections of the sunflower fields that should be and not be managed with herbicide.

Materials and methods

Sites

The study sites were two commercial sunflower fields with flat ground (average slope <1 %) situated at Monclova Farm, in Seville province (southern Spain, central co-ordinates datum WGS84: 37.528 N and 5.315 W for field 1, and 37.524 N, 5.318 W for field 2). The sunflower crops were sown on March 25th, 2014, at 6 kg ha^{-1} in rows 0.70 m apart, and emergence of the sunflower plants started 15 days after sowing. The sunflower fields had an area of approximately 1 ha each, and were naturally infested by the broad-leaved weeds *Amaranthus blitoides S. Wats* (pigweed), *Sinapis arvensis* L. (mustard) and *Convolvulus arvensis* L. (bindweed), as well as *Chenopodium album* L. (lambsquarters) in field 2. All these weed species can be controlled by the same type of herbicide. Weed and crop plants were in the principal stage 1 (leaf development, four–six true leaves, codes 14-16) from the BBCH (Biologische Bundesanstalt, Bundessortenamt und CHemische Industrie) extended scale (Meier 2001).

UAV flights: cameras and altitudes

The co-ordinates of each corner of the experimental fields were collected with GPS for planning the flight route. Then, each flight route was programmed into the UAV software to allow the UAV to attain every programmed altitude and required degree of image overlap. This imagery was collected with two different cameras mounted separately in a quadrocopter UAV, model md4-1000 (microdrones GmbH, Siegen, Germany, Fig. 1) on May 7th 2014 at two different altitudes: 30 and 60 m. A sequence of 30 % side-lap and 60 % forward-lap imagery was collected to cover the entire area of the experimental sunflower fields corresponding to each flight mission cameras and altitudes (Fig. 2). One of the cameras used was a low-cost digital visible camera, model Olympus PEN E-PM1 (Olympus Corporation, Tokyo, Japan), which acquires 12-megapixel images in true Red–Green–Blue (RGB) colour with 8-bit radiometric resolution. The other sensor was a multi-spectral camera, model Tetracam mini-MCA-6 (Tetracam Inc., Chatsworth, CA, USA), which acquires 1.3-megapixel images composed of six individual digital channels arranged in a 2 $\times$ 3 array that can acquire images with either 8-bit or 10-bit radiometric resolution. This camera has user configurable band pass filters (Andover Corporation, Salem, NH, USA) of 10-nm full-width at half maximum and centre wavelengths in the B (450 nm), G (530 nm), R (670 and 700 nm), R edge (740 nm) and near-infrared (NIR, 780 nm) spectral regions. Detailed information about the configuration of the UAV flights and specifications of the vehicle and the cameras can be found in Torres-Sánchez et al. (2013). The images taken with the visible camera were used directly after downloading to the computer, but those taken with the multi-spectral camera required pre-processing. This multi-spectral sensor acquires images in each channel in raw format and stores them separately on six individual CF cards embedded in the camera. Therefore, an alignment process was needed to group, in a single file, the six images taken at each waypoint. The Tetracam

Fig. 1 Microdrone MD4-1000 with the multi-spectral camera (6 channels) embedded flying over one the sunflower experimental fields

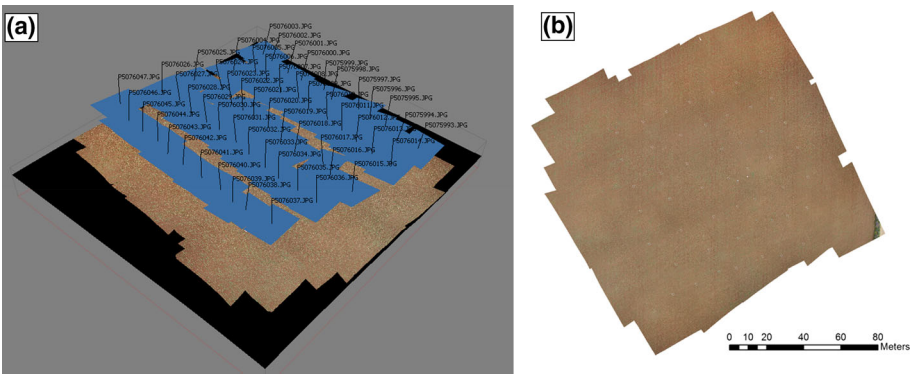

Fig. 2 **a** Screen shot of the set of overlapped images taken with UAV flying at 30 m altitude equipped with the visible still camera in field 1 (1 ha surface). *Blue rectangles* represent the relative position of every overlap image respect to the others; **b** resulting ortho-mosaicked imagery

PixelWrench 2 software (Tetracam Inc., Chatsworth, CA, USA) supplied with the multi-spectral camera was used to perform the alignment process.

In the course of the UAV flights, a barium sulphate standard spectralon® panel (Labsphere Inc., North Sutton, NH, USA) of 1 × 1 m dimension was also placed in the middle of the fields to calibrate the spectral data (Fig. 3). Digital images captured in each camera spectral channel were spectrally corrected by applying an empirical linear relationship (Hunt Jr. et al. 2010). Equation coefficients were derived by fitting digital numbers of the multi-spectral images located in the spectralon panel to the spectralon ground values.

Fig. 3 **a** Partial view of the ortho-mosaicked imagery at 30 m altitude (sunflower field 2), showing the sunflower rows, the spectralon (*white square* placed between two sunflower rows at the *bottom-left*), some patches of weed infestation and some of the 49 1×1 m *square frames*; **b** Detail of vector file created for every *square frame* (*yellow*); **c** detail of the vector file created for the sunflower crop (*green*) and weed (*violet*) classes in one the 49 *square frames*

Image mosaicking

Image mosaicking is an important task prior to image analysis and consists of the combination of the sequence of overlapped imagery by applying a process of mosaicking using Agisoft PhotoScan Professional Edition (Agisoft LLC, St. Petersburg, Russia). On the day of the UAV flights, a systematic on-ground sampling procedure was conducted, which consisted of placing 49 1×1 m sampling areas, or frames, regularly distributed throughout the two experimental fields according to a representative distribution of weed infestation in the experimental fields (Fig. 3). All the frames were georeferenced and, of the 49 frames, 12 were utilised as artificial terrestrial targets in order to perform the imagery ortho-rectification and mosaicking process. All of the 49 frames were also employed later in the validation of the OBIA procedure for the weed discrimination, as explained in the evaluation of the OBIA algorithm performance section. The mosaicking process had three principal steps for each field: (1) image alignment, i.e., the software searches for common points in the images and matches them, in addition to finding the position of the camera for each image and refining camera calibration parameters, (2) construction of image geometry based on the estimated camera positions and images themselves to produce a 3D polygon mesh representing the overflow areas was built by PhotoScan, and (3) projection of individual images once the geometry was built for orthophoto generation. The resultant ortho-mosaicked images must show a high-quality landscape metric and an accurate sunflower row matching between consecutive images in order to guarantee good performance of the subsequent segmentation and classification analyses.

OBIA algorithm

The OBIA procedure designed for the weed mapping objectives was developed using the commercial software eCognition Developer 8.9 (Trimble GeoSpatial, Munich, Germany). This OBIA procedure was based on an algorithm for weed mapping in early-season maize fields fully described in previous work by our research group (Peña et al. 2013), though that work was conducted using single imagery, whereas the procedure presented herein includes some relevant variations and upgrades related to the unique characteristics of sunflower crops. The OBIA algorithm combined object-based features such as spectral values, position, orientation and hierarchical relationships among analysis levels. The algorithm was based on the position of crop and weed plants relative to the crop rows, that is, every plant not located on the crop line was considered a weed. Therefore, the algorithm was programmed to accurately recognise and detect the crop rows by the application of a dynamic and auto-adaptive classification process, and then classified the vegetation objects outside the rows as weeds. The detailed image analysis workflow is described by Peña et al. (2013) and only the variations and improvements are described in the following steps:

(a) *Field segmentation into sub-parcels* ortho-mosaicked images taken with every camera and flight altitude were segmented into small parcels whose size is user-configurable and, in this case, was 5×5 m. Every sub-parcel was analysed individually to address the spatial and spectral variability of the crop.

(b) *Sub-parcel segmentation into objects* the sub-parcel images were sub-segmented using a multi-resolution algorithm to create homogeneous multi-pixel objects corresponding to two classes: vegetation (crop and weeds) and non-vegetation (bare soil) objects. Since these objects come from the merger of spectrally and spatially homogeneous pixels, they contain new information that was used in the next phases of the OBIA

procedure. In this study, this new information corresponded to 1, 10, 0.6, 0.4, 0.5, 0.5 for band weights, scale, color, shape, smoothness and compactness, respectively.

(c) *Vegetation objects discrimination* once the sub-parcels were segmented, the vegetation (crop and weeds) objects were discriminated from the bare soil objects. Two spectral indices were used: excess green (ExG, Woebbecke et al. 1995; Eq. 1) for the visible camera, and NDVI (Rouse et al. 1973; Eq. 2) for the multi-spectral camera because both indices enhance spectral differences of vegetation objects against the non-vegetation objects in UAV images, as previously reported by Torres-Sánchez et al. (2014). The determination of the optimal ExG and NDVI values for vegetation discrimination was conducted by an adaptation to eCognition of an iterative automatic thresholding by using Otsu's method (Otsu 1979) adapted to UAV imagery for detection of three herbaceous crops, including sunflower (Torres-Sánchez et al. 2015).

$$ExG = 2g - r - b; \quad r = \frac{R}{R+G+B} \quad g = \frac{G}{R+G+B} \quad b = \frac{B}{R+G+B} \tag{1}$$

$$NDVI = \frac{NIR - R}{NIR + R} \tag{2}$$

(d) *Sunflower crop-line detection* after classifying vegetation and bare soil objects, those corresponding to vegetation were merged to determine the crop-row structure. Crop row orientation was determined by an iterative process in which the image was successively segmented in stripes with different angles (from 0° to 180°, with 1° of increasing ratio). This segmentation in stripes was performed in a new level above the one with the classified vegetation in order to not lose this information. Finally, the crop orientation was selected according to which stripes showed a higher percentage of vegetation objects in the lower level. After a stripe was classified as a sunflower crop-line, the separation distance between rows (0.70 m) was used to mask the adjacent stripes with this distance in order to avoid classifying areas with potential high weed infestation as crop rows.

(e) *Weed-patches and weed-free maps* once the crop-rows were classified, the remaining stripes were classified as crop-row buffers (linear segments in contact with the crop rows) and non-crop areas in the upper segmentation level. Next, the hierarchical relationship between the upper and the lower segmentation levels was used to discriminate crop from weeds. The vegetation objects (in the lower segmentation level) that were located either under the crop rows or under the non-crop area (in the upper segmentation level) were classified either as sunflower or as weeds, respectively. The remaining vegetation objects located under the buffer area were classified following a criterion of minimum spectral distance, i.e., an unclassified vegetation object was assigned to the sunflower or the weed class depending on a higher degree of spectral similarity of their ExG and NDVI values to their surrounding sunflower or weed objects for the visible and the multi-spectral images, respectively.

(f) *Site-specific treatment maps* after mapping weed-patches and weed-free areas, the algorithm built a grid framework at an upper level and applied a chessboard segmentation to generate grids of user-configurable size. For example, in this investigation and according to the usual characteristics of sunflower and weed-control machinery, the grid size was 0.5 × 0.5 m. Therefore, a new hierarchical structure was generated between the grid super-objects at the upper level and the sub-objects classified as sunflower, weeds or bare soil at the lower level. Next, the site-specific treatment maps were created according to the weed coverage maps estimated previously.

(g) *Maps at several weed thresholds* the weed coverage was mapped by identifying both weed-free and weed-infested zones on the basis of seven thresholds with intervals of 2.5 from

0 % (herbicide post-emergence treatment must be applied just when there is presence or absence of weed) to 15 % (herbicide must be applied whether weed coverage >15 %) with an increase 2.5 % per threshold level. That is, seven herbicide treatment maps resulting from a given threshold value were studied for every flight altitude and camera. Both the grid dimensions and the number and thresholds of the weed infestation can be customised according to other cropping patterns and the specifications required by the herbicide spraying machinery.

Evaluation of OBIA algorithm performance

For validation purposes, the ortho-mosaicked visible imagery collected at 30 m altitude was used in both fields to quantify classification accuracy because this image had a high spatial resolution which allowed the visual identification of weeds in each of the 49 sampling frames. That is, ground reference observations were derived from the vertical remote images collected at 30 m altitude. In addition, each sampling frame was georeferenced with a DGPS and was photographed to help to visually identify the individual or group of weeds and create Fig. 3c to compare the on-ground weed infestation (observed weed density) with the outputs from image classification (estimated weed density). Therefore, two vector shape files were created, one of them containing the 49 1×1 m^2 sampling areas (Fig. 3b) and the other one including the crop and weeds existing in every frame (Fig. 3c) by using Quantum GIS software (QGIS, GNU General Public License). These vector files were then introduced into the eCognition software to obtain the percentage of surface area occupied by the three classes, i.e., sunflower, weeds and bare soil, in every square frame in order to generate the reference data. Afterwards, the first vector file was overlapped with the classified image obtained by the OBIA algorithm to calculate the relative area corresponding to each class in every frame. The accuracy of the classified images was quantified by calculating the error matrix between weed coverage mapping outputs and the field reference data in all sampling frames grouped by the weed threshold (0–15 % weed coverage) previously defined. The confusion matrix quantified the overall accuracy (OA) of the classification in each threshold (Congalton 1991).

Results and discussion

Spatial resolution and area covered by ortho-mosaicked imagery

The visible and multi-spectral cameras collected images with pixel sizes ranging from 0.0114 to 0.0162 m and from 0.0228 to 0.0327 m at flight altitudes of 30 and 60 m, respectively, as determined by a proportional relationship between imagery spatial

Table 1 Image spatial resolution, flight length and number of images per hectare as affected by flight altitude and type of camera

Camera	Flight altitude (m)	Flight length (m:s)	# Images	Pixel size (m)
Visible (RGB)[a]	30	11:56	42	0.0114
	60	5:41	12	0.0228
Multispectral (RGB + NIR)[a]	30	28:00	117	0.0162
	60	11:14	35	0.0327

[a] *RGB* red, blue green, near-infrared

resolution and flight altitude (Table 1). Furthermore, slight changes in flight altitude during the flight are critical for low altitude image acquisition because these variations can cause important differences in the ortho-image spatial resolution. Weeds can be present in the field as small or large patches, so the spatial resolution of the image must be considered accordingly (Fig. 4). If the objective is the detection of small weed patches, the pixel size could be 0.01–0.03 m which corresponds to flight altitudes of 30 and 60 m for the visible camera and 30 m for the multi-spectral camera. However, when a weed patch is larger, the UAV images could have a pixel size larger than 0.03 m, which corresponds to 60 m flight altitude in the multi-spectral camera.

The number of images and the flight length needed to cover the entire study area increased from 42 to 117 images and from 12 to 28 min for the visible and the multi-spectral camera, respectively, at 30 m altitude. A similar trend was observed at 60 m altitude. The different spatial resolutions and area covered for the visible and multi-spectral cameras at the same flight altitude resulted from differences in the technical specifications of each camera; i.e., the camera's focal length and sensor size affect the extent of area covered for a given sensor, and the pixel size of the sensor (measured in μm) determines the relationship between flight altitude and spatial resolution for a given sensor. Therefore, a decrease in the flying altitude reduces the area covered by each single image, which results in an increase in both the sequence of images and the complexity of the image mosaicking procedure to obtain an ortho-image covering the entire study area. Considering these relationships between flight characteristics and camera types, the first decision to

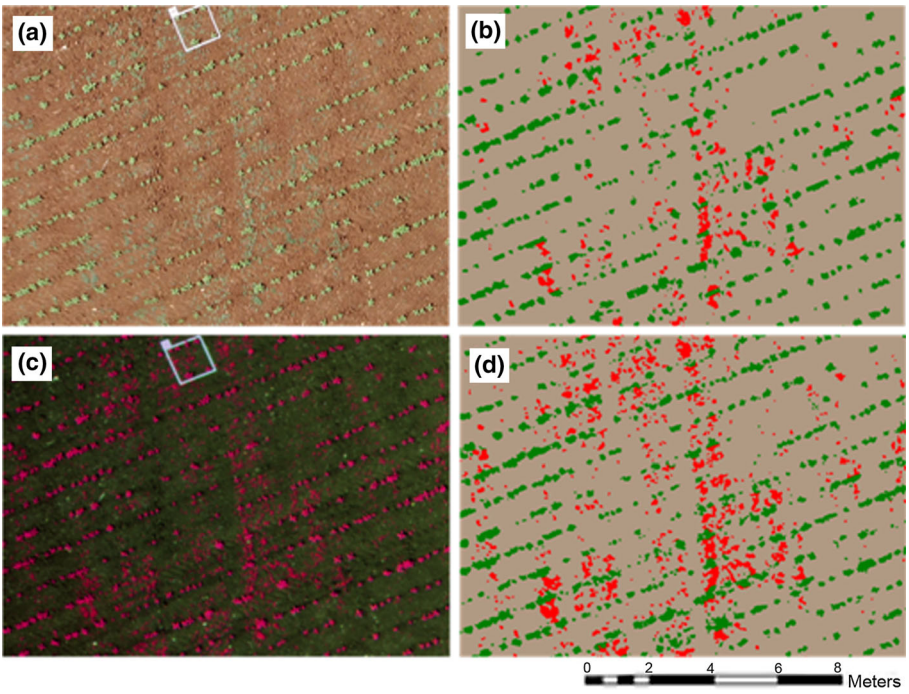

Fig. 4 **a** Illustration of the ortho-mosaicked image taken with the visible camera at 30 m altitude, and **b** corresponding weed seedling map using OBIA (*green* sunflower rows; *red* weeds; *grey* bare soil); **c** illustration of the ortho-mosaicked image taken with the multi-spectral camera at 30 m altitude, and **d** corresponding weed seedling map using OBIA

make when the user defines the flight program is which combination of flight altitude and camera type is ideal to keep the image spatial and spectral quality consistent to ensure weed detection and minimise the operating time, given potential UAV battery limitations. These considerations need to be addressed to design prescription control maps because early SSWM requires high accuracy geo-referencing in agreement to the details of the crop, weeds and soil background classes when both kind of plants are at very similar phenological stages and a repeating crop pattern is present.

Classification of sunflower crop rows

Sunflower crop rows were detected and mapped with 100 % accuracy in the ortho-mosaics, at all flight altitudes and camera types, using the OBIA algorithm (Fig. 4). This was due not only to the performance of this procedure but also to the high matching of crop-line continuity of ortho-imagery during the mosaicking process. If mosaics were not accurate enough, crop rows would appear broken, incorrectly geo-referenced and consequently, moved, which would affect further OBIA classification. This algorithm was upgraded to incorporate the special characteristics of sunflower crops and now includes relevant variations to previous versions, e.g., imagery was mosaicked to study the whole fields to optimise the image analysis, and weed thresholds were considered in the construction of site-specific treatment maps. Other authors have mosaicked imagery from other row crops such as corn, although the objective was to determine the effect of topography on the rate of cross-pollination (Haarbrink 2008). However, they found that obtaining an accurate ortho-image was difficult, but they did not need to map crop rows. Therefore, one of the critical results of the work reported here was the robustness of both the mosaicking and OBIA methods developed for crop-row classification and mapping. This is relevant for the successful detection of the vegetation objects referred to weeds placed in the inter-row areas.

Effect of cameras and flight altitudes on mapping of weed-patches and weed-free areas

The accuracy of weed-patch discrimination, as affected by flight altitude and camera using seven threshold values, are shown in Fig. 5 for both sunflower fields. The classification was over grid units, not over pixels, therefore the accuracy was the percentage of frames

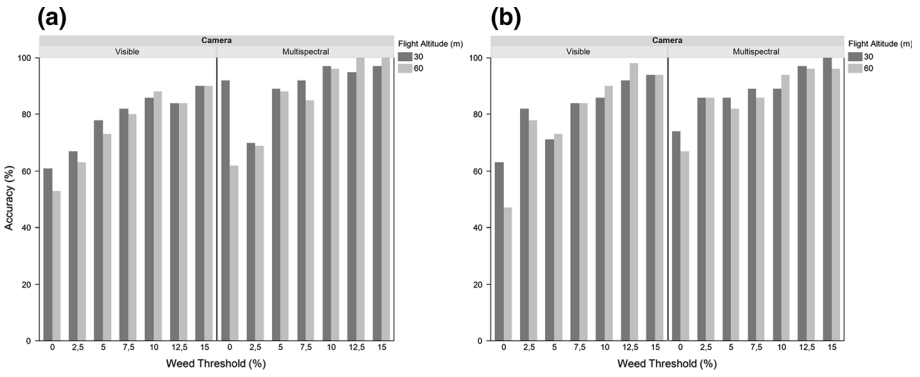

Fig. 5 Accuracy (%) of weed maps according to seven weed thresholds for the images collected with the visible and multi-spectral cameras collected at 30 and 60 m altitude for **a** field 1, **b** field 2

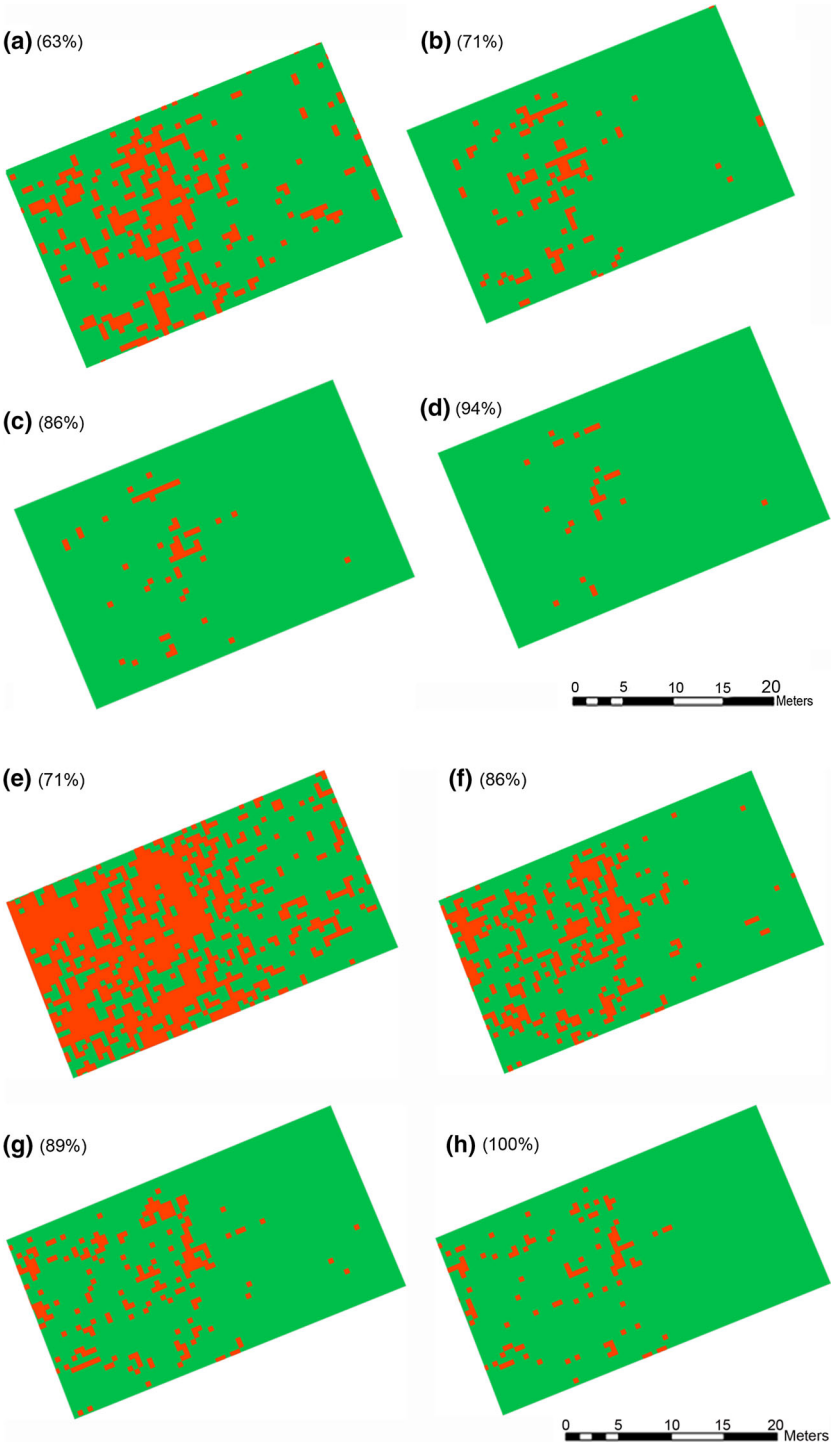
(a) (63%)
(b) (71%)
(c) (86%)
(d) (94%)
0 5 10 15 20
Meters
(e) (71%)
(f) (86%)
(g) (89%)
(h) (100%)
0 5 10 15 20
Meters

◀**Fig. 6** Several examples of maps showing the herbicide application area (*black square*) obtained for 30 m altitude, and using visible camera (*four upper figures*) and multi-spectral camera (*four bottom figures*) for field 2 corresponding to four weed thresholds: **a** and **e** 0 %; **b** and **f** 5 %; **c** and **g** 10 %; **d** and **h** 15 %. The accuracy of every weed map is shown in *parentheses*

correctly classified, i.e., the number of correct frames as a percentage of the total number of sampling frames. The threshold corresponding to zero means that the OBIA algorithm detects simply the presence or absence of weeds, that is, a percentage of weeds greater than zero was detected in the inter-row area, and consequently, all these weeds must be treated. A threshold of 15 % means that at least 15 % of the inter-row area of every frame was infested; if a lower weed infestation is detected and mapped, no treatment should be applied.

Both sunflower fields showed similar results and trends. Higher accuracies were observed with the multi-spectral camera at both flight altitudes, the highest (approximately 100 %) was recorded for 15 % threshold, although satisfactory results from 2.5 to 5 % thresholds were also obtained with accuracies higher than 85 % for fields 2 and 1, respectively. The lowest accuracies (ranging from 50 to 60 %) were achieved with the visible camera at any flight altitude and 0 % of threshold value although, according to Thomlinson et al. (1999) who standardised the overall accuracy of 85 % for minimum established values, acceptable accuracies were also recorded from a 7.5 % threshold for both fields. Best accuracies were achieved for the higher thresholds because, normally, they imply the presence of larger weed patches which are more easily detected by the OBIA algorithm. When analysing frames with only 2.5 % weed infestation, the most common situation is that the weed patches are very small, and consequently, they are more difficult to discriminate. Analysing the flight altitude, accuracies for the images taken with the visible camera at 60 m were higher than at 30 m for 10 % weed threshold for field 1 and 12.5 % in field 2. A similar trend was observed with the multi-spectral camera. Therefore, a higher altitude corresponds to higher accuracies for high weed thresholds in both fields. This indicated that, in a sunflower field with a high weed infestation, the UAV could be programmed to fly at 60 m altitude and perform better than at 30 m, because the weed map would have a satisfactory accuracy, while requiring fewer images per ha, thus improving both the flight time and the mosaicking process.

Traditionally, ExG and NDVI indices have been widely used in mapping vegetation (190,000 and 330,000 results in Google for "remote sensing" plus "Excess Green", and "NDVI", respectively; accessed August 2015), however, they were quite limited for mapping crop-rows and weeds using pixel-based-image-analysis in the preliminary image analyses (data not shown). This is because reflectance data are sensitive to canopy cover, and spectral data from crop and weed plants at early phenological stage are rather similar and difficult to discern. The OBIA procedure developed has the ability to build objects using several criteria of homogeneity, in addition to spatially accurate information (e.g., position, orientation, hierarchical relationships among image analysis levels). Figure 6 displays several illustrative examples of early, site-specific, post-emergence grid maps for different scenarios at 30 m flight altitude, using both visible and multi-spectral cameras. They also contain four thresholds and the spatial distributions of treated and untreated grids. For a wider weed threshold, a lower weed-patch area was observed, and vice versa, consequently, the threshold value has a direct effect on the percentage of the field to be treated (Fig. 7). The herbicide savings obtained were relevant for both cameras and altitudes in both fields, although they were higher in field 2 due to the lower degree of weed

infestation. The percentage of treated area was calculated to be higher when using the multi-spectral camera because the weed patches were better discriminated and the maps generated were more accurate than those from the visible camera.

That is, some weed patches present in the field were not correctly classified with imagery from the visible camera, and as a result, no treatment was indicated. For example, using the multi-spectral camera at 30 m altitude, a range of 3–23 % of the field (i.e., 77 and 97 % of untreated area) could be treated for weed thresholds from 0 to 15 %, corresponding to accuracies ranging from 74 to 100 % for field 2. On the other hand, using the visible camera at 30 m, a range of 3–9 % of the field (i.e., 92 and 97 % of untreated area) could be treated for weed thresholds from 0 to 15 %, corresponding to accuracies from 63 to 94 % for field 1. As Fig. 6 shows, there are some parts of the fields where there were clearly weed-free zones and where site-specific weed control equipment was not needed, allowing not only the potential reduction of herbicide applications but also the optimisation of fuel, field operating time and cost. Currently, accurate site-specific equipment for farmers to implement site-specific weed management is available. In addition, collaborative efforts have been conducted to develop autonomous and robotic tractors carrying different implements for site-specific control of weeds and other pests using a high-level decision-making system. This system was designed to accurately manage the type of herbicide or dose level for other pesticides according to a prescription map (Pérez-Ruiz et al. 2015).

The spatial structure was also different in both fields, i.e., the weeds were distributed in patches across all of field 1, but were more localised in a part of field 2. The extent of the weed-infested area and its spatial distribution, as well as the adoption of weed thresholds,

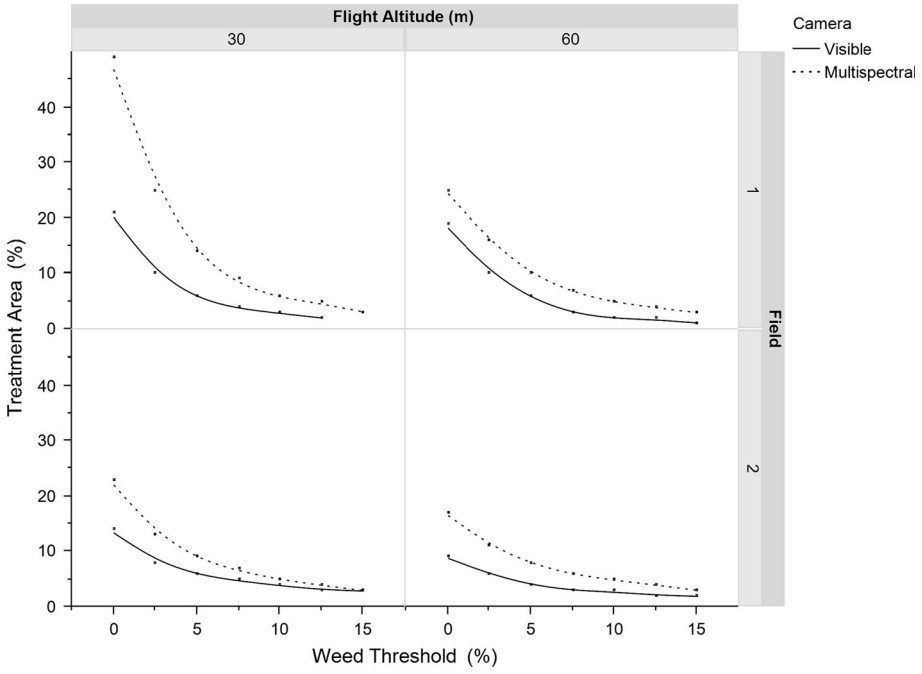

Fig. 7 Percentage of field surface requiring weed control in both sunflower fields based on seven weed thresholds according to flight altitudes and cameras

are crucial for the design and implementation of early SSWM. In addition, Gibson et al. (2004) stated that farmers would choose to treat weed-free areas rather than assume the risk of allowing weeds to go untreated, and Czapar et al. (1997) reported several reasons to consider the use of thresholds, such as crop competition, harvesting problems, weed seed production and seed bank replenishment, time required to survey fields or even general field appearance. Analysing this latter work, the time spent to explore fields was perceived to be a limitation for the acceptance of weed thresholds by 6 % of growers, while 26 % of dealers and 39 % of farm managers also identified it as a restraint. This could be overcome by using the technology presented here based on a UAV since the time spent to acquire 1 ha of sunflower area was less than half an hour for any of the flight altitudes and cameras (Table 1). Of course, the processing time for image analysis would have to also be considered, although once the algorithm is developed, this time would be minimal for successive use in as many sunflower fields as required. Field appearance was identified by 75 % of the dealers and 36 % of growers as an important limitation. This can be relevant if weeds of medium to large size are present in the sunflower fields, as was the case in this study. Pigweed and lambsquarters are considered large weeds, while mustard and bindweed are medium weeds according to the SEMAGI expert system developed for weed management in sunflower (Castro-Tendero and García-Torres 1995). These authors evaluated herbicide selection according to potential yield reduction from multi-species weed infestations by assigning three size categories (small, medium and large) to weeds and relating the percentage of sunflower losses to weed density and weed biomass. They concluded that the subjective evaluation of farmers for weed infestation assessment usually considers the size of the weed for herbicide decisions and this is in agreement with the results reported by Czapar et al. (1997). Using SEMAGI and geostatistical tools, Jurado-Expósito et al. (2003) reported the usefulness of weed infestation maps for identifying the area exceeding the economic threshold to plan site-specific spraying strategies; they obtained 61 % herbicide reduction. Therefore, the site-specific treatment maps considering the different thresholds shown in Fig. 6 could help farmers to decide on early SSWM operations without forgetting the subjective evaluation of their fields as an important component of their decision making. For example, according to the previously mentioned limitations found by land owners, it seems unlikely that they would choose the 15 % threshold keeping treated approximately 5 % of both fields (Fig. 6) and untreated most of the fields, particularly when these areas subjectively would appear highly infested due to large size of weeds such as lambsquarters or pigweeds.

Current investigations are focusing on improving the OBIA algorithm when a number of specific field conditions, such as curved crop rows, are present in the fields.

Conclusions

Because the spatial structure of patchy distribution of weeds allows mapping of infested and un-infested areas, the objectives were to detect patches of weeds at early phenological stages using UAV imagery and to design a timely and efficient weed control program based on site-specific herbicide treatments according to weed cover. A UAV equipped with RGB or multi-spectral cameras flying at 30 and 60 m altitude was used to acquire a set of overlapped images. The spatial resolution of the image, area covered by each image and flight timing were very sensitive to the flight altitude. At a lower altitude using the visible camera, the UAV captured slightly finer spatial resolution imagery than at the same

altitude using the multi-spectral camera. However, the number of images needed to cover the entire field at 30 m altitude with the visible camera was much lower than for the multi-spectral camera, showing that it may be a limiting factor due to potential UAV energy limitations. The overlapped images were ortho-mosaicked to generate imagery at very-high spatial resolutions (pixels ranging from 0.0114 to 0.0327 m). An accurate and automated OBIA procedure was developed to detect and map bare soil, crop-rows and weeds. Accurate site-specific herbicide treatment maps were created according to different factors: flight altitudes, camera types and weed thresholds, and then relevant herbicide savings were calculated. This information can help to balance spatial resolution, which depends on flying altitude and type of camera with decision-making to calculate herbicide requirements and plan the overall weed management operations.

Acknowledgments This research was partially financed by the RECUPERA 2020 Project (Agreement CSIC-Spanish MINECO and EU-FEDER funds). Research of Mr. Torres-Sánchez, Dr. de Castro and Dr. Peña was financed by the FPI, the JAE-predoc (CSIC-FEDER) and Ramón y Cajal Programs, respectively.

References

Blaschke, T. (2010). Object based image analysis for remote sensing. *ISPRS Journal of Photogrammetry and Remote Sensing, 65*, 2–16.

Carranza, P., Saavedra, M., & Gacría-Torres, L. (1995). *Ridolfia segetum* Moris. competition with sunflower (*Helianthus annuus* L.). *Weed Research, 35*, 369–375.

Castro-Tendero, A. J., & García-Torres, L. (1995). SEMAGI—an expert system for weed control decision making in sunflowers. *Crop Protection, 14*, 543–548.

Congalton, R. G. (1991). A review of assessing the accuracy of classifications of remotely sensed data. *Remote Sensing of Environment, 37*, 35–46.

Czapar, G. F., Curry, M. P., & Wax, L. M. (1997). Grower acceptance of economic thresholds for weed management in Illinois. *Weed Technology, 11*, 828–831.

De Castro, A. I., Jurado-Expósito, M., Peña-Barragán, J. M., & López-Granados, F. (2012). Airborne multi-spectral imagery for mapping cruciferous weeds in cereal and legume crops. *Precision Agriculture, 13*, 302–321.

De Castro, A. I., López-Granados, F., Peña-Barragán, J. M., & Jurado-Expósito, M. (2013). Broad-scale cruciferous weed patches classification in winter wheat using QuickBird imagery for in-season site-specific control. *Precision Agriculture, 14*, 392–417.

FAO (2015). http://faostat3.fao.org/faostat-gateway/go/to/home/E. Accessed 16 June 2014.

García-Torres, L., López-Granados, F., & Castejón-Muñoz, M. (1994). Preemergence herbicides for the control of broomrape (*Orobanche cernua* Loefl.) in sunflower (*Helianthus annuus* L.). *Weed Research, 34*, 395–402.

Gibson, K. D., Dirks, R., Medlin, C. R., & Johnston, L. (2004). Detection of weed species in soybean using multispectral digital images. *Weed Technology, 18*, 742–749.

Gómez-Candón, D., De Castro, A. I., & López-Granados, F. (2014). Assessing the accuracy of mosaics from unmanned aerial vehicle (UAV) imagery for precision agriculture purposes. *Precision Agriculture, 15*, 44–56.

Gutiérrez-Peña, P. A., López-Granados, F., Peña-Barragán, J. M., Jurado-Expósito, M., Gómez-Casero, M. T., & Hervás-Martínez, C. (2008). Mapping sunflower yield as affected by *Ridolfia segetum* patches and elevation by applying evolutionary product unit neural networks to remote sensed data. *Computers and Electronics in Agriculture, 60*, 122–132.

Haarbrink, R. B., & Eisenbeiss, H. (2008). Accurate DSM production from unmanned helicopter systems. *The International Archives of the Photogrammetry, Remote Sensing and Spatial Information Sciences, XXXVII*(Part B1), 1259–1264.

Horizon (2020) http://ec.europa.eu/programmes/horizon2020/. Accessed 16 June 2015.

Hunt, E. R, Jr., Hively, W. D., Fujikawa, S. J., Linden, D. S., Daughtry, C. S. T., & McCarty, G. W. (2010). Acquisition of NIR-green-blue digital photographs from unmanned aircraft for crop monitoring. *Remote Sensing, 2*, 290–305.

Jurado-Expósito, M., López-Granados, F., García-Torres, L., García-Ferrer, A., Sánchez de la Orden, M., & Atenciano, S. (2003). Multi-species weed spatial variability and site-specific management maps in cultivated sunflower. *Weed Science, 51*, 319–328.

Jurado-Expósito, M., López-Granados, F., González-Andújar, J. L., & García-Torres, L. (2005). Characterizing population rate of *Convolvulus arvensis* in wheat-sunflower no-tillage systems. *Crop Science, 45*, 2106–2112.

Lambers, K., Eisenbeiss, H., Sauerbier, M., Kupferschmidt, D., Gaisecker, Th, Sotoodeh, S., et al. (2007). Combining photogrammetry and laser scanning for the recording andmodelling of the late intermediate period site of Pinchango Alto, Palpa, Peru. *Journal of Archaeological Science, 34*, 1702–1712.

Li, Ch-ch, Zhang, G.-S., Lei, T.-J., & Gong, A.-D. (2011). Quick image-processing method of UAV without control points data in earthquake disaster area. *Transactions Nonferrous Metals Society of China, 21*, s523–s528.

Longchamps, L., Panneton, B., Simard, M. J., & Leroux, G. D. (2014). An imagery-based weed cover threshold established using expert knowledge. *Weed Science, 62*, 177–185.

López-Granados, F. (2011). Weed detection for site-specific weed management: Mapping and real-time approaches. *Weed Research, 51*, 1–11.

MAGRAMA (2015). Ministerio Agricultura, Alimentación y Medioambiente. http://www.magrama.gob.es/es/estadistica/temas/default.aspx. Accessed 16 June 2015 (in Spanish).

Meier, U. (2001). *Growth stages of mono- and dicotyledonous plants. BB Monograph*. Federal Biological Research Centre for Agriculture and Forestry. http://www.jki.bund.de/fileadmin/dam_uploads/_veroeff/bbch/BBCH-Skala_englisch.pdf. Accessed 16 June 2015.

Molinero-Ruiz, L., García-Carneros, A. B., Collado-Romero, M., Rarancius, S., Domínguez, J., & Melero-Vara, J. (2014). Pathogenic and molecular diversity in highly virulent populations of the parasitic weed *Orobanche cumana* (sunflower broomrape) from Europe. *Weed Research, 54*, 87–98.

Otsu, N. (1979). A threshold selection method from gray-level histograms. *IEEE, Man, and Cybernetics Society, 9*, 62–66.

Peña, J. M., Torres-Sánchez, J., de Castro, A. I., Kelly, M., & López-Granados, F. (2013). Weed mapping in early-season maize fields using object-based analysis of unmanned aerial vehicle (UAV) images. *PLoS One, 8*, e77151.

Pérez-Ruiz, M., Gonzalez-de-Santos, P., Ribeiro, A., Fernandez-Quintanilla, C., Peruzzi, A., Vieri, M., et al. (2015). Highlights and preliminary results for autonomous crop protection. *Computers and Electronics in Agriculture, 110*, 150–161.

Rouse, J. W., Haas, R. H., Schell, J. A. & Deering, D. W. (1973). Monitoring vegetation systems in the Great Plains with ERTS. In: *Proceedings of the Earth Resources Technology Satellite Symposium* NASA SP-351, (vol 1, pp. 309–317). Washington, DC.

Swanton, C. J., Weaver, S., Cowan, P., Van Acker, R., Deen, W., & Shreshta, A. (1999). Weed thresholds: Theory and applicability. *Journal of Crop Production, 2*, 9–29.

Thomlinson, J. R., Bolstad, P. V., & Cohen, W. B. (1999). Coordinating methodologies for scaling land-cover classification from site-specific to global: Steps toward validating global maps products. *Remote Sensing of Environment, 70*, 16–28.

Torres-Sánchez, J., López-Granados, F., de Castro, A. I., & Peña-Barragán, J. M. (2013). Configuration and specifications of an unmanned aerial vehicle (UAV) for early site specific weed management. *PLoS One, 8*, e58210.

Torres-Sánchez, J., López-Granados, F., & Peña-Barragán, J. M. (2015). An automatic object-based method for optimal thresholding in UAV images: Application for vegetation detection in herbaceous. *Computers and Electronics in Agriculture, 114*, 43–52.

Torres-Sánchez, J., Peña-Barragán, J. M., de Castro, A. I., & López-Granados, F. (2014). Multi-temporal mapping of the vegetation fraction in early-season wheat fields using images from UAV. *Computers and Electronics in Agriculture, 103*, 104–113.

Woebbecke, D. M., Meyer, G. E., Von Bargen, K., & Mortensen, D. A. (1995). Color indices for weed identification under various soil, residue, and lighting conditions. *Transactions of the ASAE, 38*(259–269), 28.

Zhang, C., & Kovacs, J. (2012). The application of small unmanned aerial systems for precision agriculture: A review. *Precision Agriculture, 13*, 693–712.